# Chapter 2

# The interferometer principles

## Stéphane Guilloteau

IRAM, 300 rue de la Piscine, F-38406 Saint Martin d'Hères

This lecture presents the principle of the heterodyne interferometer. An heterodyne interferometer is composed of antennas (described in A.Greve lecture 1), receivers (described in B.Lazareff lecture 3), a correlator (described in H.Wiesemeyer lecture 4) and an awful lot of cables and connections. This lecture only describes the basic principles; a more complete description, including subtleties due to multiple frequency conversions and digital delay lines, is given in R.Lucas lecture 5.

## 2.1 Basic principle

The antenna produces a Voltage proportional to the linear superposition of the incident electric field pattern. For a simple monochromatic case:

$$U(t) = E\cos(2\pi\nu t + \Phi) \tag{2.1}$$

In the receiver, a mixer superimposes the field generated by a local oscillator to the antenna output.

$$U_{LO}(t) = Q\cos(2\pi\nu_{LO} t + \Phi_{LO}) \tag{2.2}$$

The mixer is a non-linear element (diode) whose output is

$$I(t) = a_0 + a_1(V(t) + V_{LO}(t)) + a_2(V(t) + V_{LO}(t))^2 + a_3(V(t) + V_{LO}(t))^3 + ... \tag{2.3}$$

The second order (quadratic) term of Eq.3 can be expressed as

$$
\begin{aligned}
I(t) = \quad & ... \\
& + \ a_2 E^2 \cos^2(2\pi\nu t + \Phi) \\
& + \ 2a_2 EQ\cos(2\pi\nu t + \Phi)\cos(2\pi\nu_{LO} t + \Phi_{LO}) \\
& + \ a_2 Q^2 \cos^2(2\pi\nu_{LO} t + \Phi_{LO}) \\
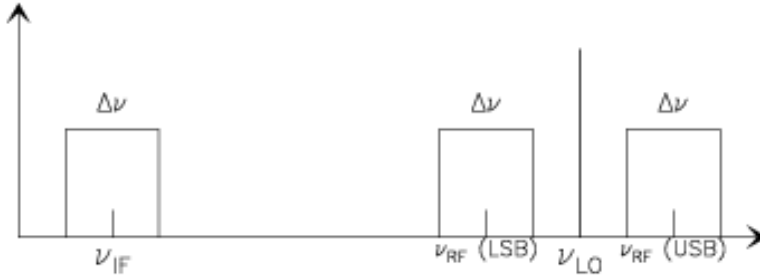& + \ ...
\end{aligned}
\tag{2.4}
$$

Figure 2.1: Relation between the IF, RF and local oscillator frequencies in an heterodyne system

Developping the product of the two cosine functions, we obtain

$$
\begin{aligned}
I(t) = \quad & \dots \\
+ \quad & a_2 E Q \cos(2\pi(\nu + \nu_{LO})t + \Phi + \Phi_{LO}) \\
+ \quad & a_2 E Q \cos(2\pi(\nu - \nu_{LO})t + \Phi - \Phi_{LO}) \\
+ \quad & \dots
\end{aligned}
\tag{2.5}
$$

There are obviously other terms in $2\nu_{LO}$, $2\nu$, $3\nu_{LO} \pm \nu$, etc $\dots$ in the above equation, as well as terms at very different frequencies like $\nu$, $3\nu$, etc $\dots$

By inserting a filter at the output of the `mixer`, we can select only the term such that

$$
\nu_{IF} - \Delta\nu/2 \leq |\nu - \nu_{LO}| \leq \nu_{IF} + \Delta\nu/2
\tag{2.6}
$$

where $\nu_{IF}$, the so-called *Intermediate Frequency*, is a frequency which is significantly different from than the original signal frequency $\nu$ (which is often called the *Radio Frequency* $\nu_{RF}$).

Hence, after mixing and filtering, the output of the `receiver` is

$$
I(t) \quad \propto \quad E Q \cos(2\pi(\nu - \nu_{LO})t + \Phi - \Phi_{LO})
\tag{2.7}
$$

$$
or
$$

$$
I(t) \quad \propto \quad E Q \cos(2\pi(\nu_{LO} - \nu)t - \Phi + \Phi_{LO})
\tag{2.8}
$$

i.e.

- changed in frequency: $\nu \to \nu - \nu_{LO}$ or $\nu \to \nu_{LO} - \nu$

- proportional to the original electric field of the incident wave: $\propto E$

- with a phase relation with this electric field: $\Phi \to \Phi - \Phi_{LO}$ or $\Phi \to \Phi_{LO} - \Phi$

- proportional to the `local oscillator` voltage: $\propto Q$

The frequency change, usually towards a lower frequency, allows to select $\nu_{IF}$ such that amplifiers and transport elements are easily available for further processing. The mixer described above accepts simultaneously frequencies which are (see Fig.2.1)

- higher than the `local oscillator` frequency.
  This is called Upper Side Band (USB) reception

- lower than the `local oscillator` frequency.
  This is called Lower Side Band (LSB) reception

and cannot *a priori* distinguish between them. This is called Double Side Band (DSB) reception. Some receivers are actually insensitive to one of the frequency range, either because a filter has been placed at the receiver input, or because their response is very strongly frequency dependent. Such receivers are called Single Side Band (SSB) receivers.
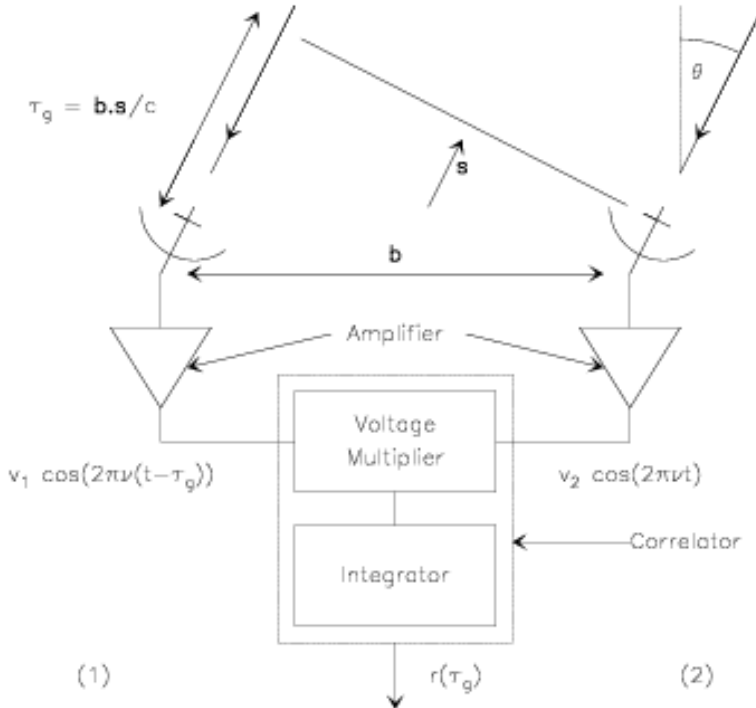
Figure 2.2: Schematic Diagram of a two-element interferometer

An important property of the receiving system expressed by Eq.2.8 is that the sign of the phase is changed for LSB conversion. This property can be easily retrieved recognizing that the **Frequency $\nu$ is the time derivative of the Phase $\Phi$**. Assume the phase varies linearly with time:

$$\begin{aligned} \Phi(t) &= 2\pi n t \\ n &= \frac{1}{2\pi} \frac{d\Phi}{dt} \end{aligned} \qquad (2.9)$$

In this case, the signal

$$\begin{aligned} I(t) &\propto \cos(2\pi\nu t + \Phi(t)) \\ &\propto \cos(2\pi(\nu + n)t) \end{aligned} \qquad (2.10)$$

is just another monochromatic signal with slightly shifted frequency.

## 2.2 The Heterodyne Interferometer

Figure 2.2 is a schematic illustration of a 2-antenna heterodyne interferometer.

*Let us forget the frequency conversion for some time, i.e. assume $\nu_{IF} = \nu_{RF}$...*

The input (amplified) signals from 2 elements of the interferometer are processed by a `correlator`, which is just a voltage multiplier followed by a time integrator. With one incident plane wave, the output $r(t)$ is

$$r(t) = < v_1 \cos(2\pi\nu(t - \tau_g(t))) v_2 \cos(2\pi\nu t) > = v_1 v_2 \cos(2\pi\nu\tau_g(t)) \qquad (2.11)$$
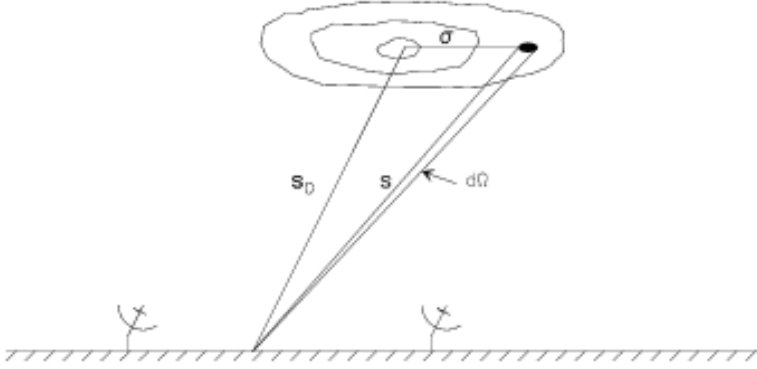
Figure 2.3: Position vectors used for the expression of the interferometer response to an extended source, schematically represented by the iso-contours of the sky brightness distribution.

where $\tau_g$ is obviously the geometrical delay,

$$\tau_g(t) = (\mathbf{b}.\mathbf{s})/c \qquad (2.12)$$

As $\tau_g$ varies slowly because of Earth rotation, $r(t)$ oscillates as a cosine function, and is thus called the *fringe pattern*. As we had shown before that $v_1$ and $v_2$ were proportional to the electric field of the incident wave, the correlator output (fringe pattern) is thus proportional to the power of the wave.

### 2.2.1   Source Size Effects

The signal power received from a sky area $d\Omega$ in direction $\mathbf{s}$ is (see Fig.2.3 for notations) $A(\mathbf{s})I(\mathbf{s})d\Omega d\nu$ over bandwidth $d\nu$, where $A(\mathbf{s})$ is the antenna power pattern (assumed identical for both elements, more precisely $A(\mathbf{s}) = A_i(\mathbf{s})A_j(\mathbf{s})$ with $A_i$ the voltage pattern of antenna $i$), and $I(\mathbf{s})$ is the sky brightness distribution

$$dr = A(\mathbf{s})I(\mathbf{s})d\Omega d\nu \cos(2\pi\nu\tau_g) \qquad (2.13)$$

$$r = d\nu \int_{Sky} A(\mathbf{s})I(\mathbf{s})\cos(2\pi\nu\mathbf{b}.\mathbf{s}/c)d\Omega \qquad (2.14)$$

Two implicit assumptions have been made in deriving Eq.2.14. We assumed incident plane waves, which implies that the source must be in the far field of the interferometer. We used a linear superposition of the incident waves, which implies that the source must be spatially incoherent. These assumptions are quite valid for most astronomical sources, but may be violated under special circumstances. For example VLBI observations of solar system objects would violate the first assumption, while observations of celestial masers could (in theory) violate the second one.

When the interferometer is tracking a source in direction $\mathbf{s}_o$, with $\mathbf{s} = \mathbf{s}_o + \sigma$

$$r = d\nu \cos(2\pi\nu\mathbf{b}.\mathbf{s}_o/c) \int_{Sky} A(\sigma)I(\sigma)\cos(2\pi\nu\mathbf{b}.\sigma/c)d\Omega$$

$$- d\nu\sin(2\pi\nu\mathbf{b}.\mathbf{s}_o/c) \int_{Sky} A(\sigma)I(\sigma)\sin(2\pi\nu\mathbf{b}.\sigma/c)d\Omega \qquad (2.15)$$

We define the *Complex Visibility*

$$V = |V|e^{j\Phi_V} = \int_{Sky} A(\sigma)I(\sigma)e^{(-2i\pi\nu\mathbf{b}.\sigma/c)}d\Omega \qquad (2.16)$$

which resembles a Fourier Transform...

We thus have

$$
\begin{aligned}
r &= d\nu \left(\cos(2\pi\nu\mathbf{b}.\mathbf{s}_o/c)|V|\cos(\Phi_V) - \sin(2\pi\nu\mathbf{b}.\mathbf{s}_o/c)|V|\sin(\Phi_V)\right) \\
&= d\nu|V|\cos(2\pi\nu\tau_g - \Phi_V)
\end{aligned} \tag{2.17}
$$

i.e. the `correlator` output is proportional to the amplitude of the visibility, and contains a phase relation with the visibility.

### 2.2.2 Finite Bandwidth

Integrating over $d\nu$,

$$
R = \frac{1}{\Delta\nu} \int_{\nu_0 - \Delta\nu/2}^{\nu_0 + \Delta\nu/2} |V|\cos(2\pi\nu\tau_g - \Phi_V)d\nu \tag{2.18}
$$

Using $\nu = \nu_0 + n$

$$
\begin{aligned}
R &= \frac{1}{\Delta\nu} \int_{-\Delta\nu/2}^{\Delta\nu/2} |V|\cos(2\pi\nu_0\tau_g - \Phi_V + 2\pi n\tau_g)dn \tag{2.19} \\
&= \frac{1}{\Delta\nu} [\int_{-\Delta\nu/2}^{\Delta\nu/2} |V|\cos(2\pi\nu_0\tau_g - \Phi_V)\cos(2\pi n\tau_g)dn \\
&\quad - \int_{-\Delta\nu/2}^{\Delta\nu/2} |V|\sin(2\pi\nu_0\tau_g - \Phi_V)\sin(2\pi n\tau_g)dn] \tag{2.20} \\
&= \frac{1}{\Delta\nu}|V|\cos(2\pi\nu_0\tau_g - \Phi_V) \left[\sin(2\pi n\tau_g)\right]_{-\Delta\nu/2}^{\Delta\nu/2} \frac{1}{2\pi\tau_g} \\
&\quad + \frac{1}{\Delta\nu}|V|\sin(2\pi\nu_0\tau_g - \Phi_V) \left[\cos(2\pi n\tau_g)\right]_{-\Delta\nu/2}^{\Delta\nu/2} \frac{1}{2\pi\tau_g} \tag{2.21} \\
&= |V|\cos(2\pi\nu_0\tau_g - \Phi_V)\frac{\sin(\pi\Delta\nu\tau_g)}{\pi\Delta\nu\tau_g} \tag{2.22}
\end{aligned}
$$

The fringe visibility is attenuated by a $\sin(x)/x$ envelope, called the bandwidth pattern, which falls off rapidly. A 1% loss in visibility is obtained for $|\Delta\nu\tau_g| \simeq 0.078$, or with $\Delta\nu = 500$MHz and a baseline length $b = 100$m, when the zenith angle $\theta$ (defined in Fig.2.3) is 2 arcmin only. Thus, the ability to track a source for a significant hour angle coverage requires proper compensation of the geometrical delay when a finite bandwidth is desired.

## 2.3 Delay Tracking and Frequency Conversion

To compensate for the geometrical delay variations, delay lines with mirrors (as in optics...) would be completely impractical given the required size of the mirrors. The compensating delay is thus performed electronically after one (or several) frequency conversion(s), as illustrated in Fig.2.4. This can be implemented either by switching cables with different lengths, or in a more sophisticated way, by using shift memories after digital sampling of the signal in the correlator. Apart for a few details (see R.Lucas lecture), the principle remains identical.

In the case presented in Fig.2.4, for USB conversion, the phase changes of the input signals before reaching the correlator are

$$
\begin{aligned}
\Phi_1 &= 2\pi\nu\tau_g = 2\pi(\nu_{LO} + \nu_{IF})\tau_g \tag{2.23} \\
\Phi_2 &= 2\pi\nu\tau_i + \Phi_{LO} \tag{2.24}
\end{aligned}
$$

Introducing $\Delta\tau = \tau_g - \tau_i$ as the delay tracking error, the correlator output is

$$
\begin{aligned}
r &= A_o|V|\cos(\Phi_1 - \Phi_2 - \Phi_V) \\
USB \quad r &= A_o|V|\cos(2\pi(\nu_{LO}\tau_g + \nu_{IF}\Delta\tau) - \Phi_V - \Phi_{LO}) \\
LSB \quad r &= A_o|V|\cos(2\pi(\nu_{LO}\tau_g - \nu_{IF}\Delta\tau) - \Phi_V - \Phi_{LO})
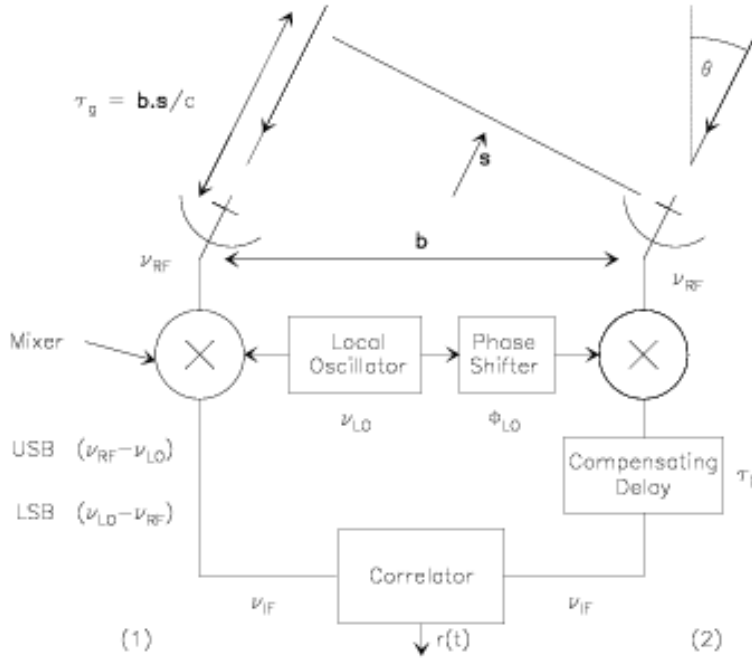\end{aligned} \tag{2.25}
$$

Figure 2.4: 2-element heterodyne interferometer with delay tracking after frequency conversion

When the two sidebands are superposed,

$$DSB \quad r \quad = \quad 2A_o|V|\cos(2\pi(\nu_{LO}\tau_g - \Phi_V - \Phi_{LO}))\cos(2\pi\nu_{IF}\Delta\tau) \tag{2.26}$$

i.e. the amplitude is modulated by the delay tracking error. The tolerance can be exceedingly small. For example, at Plateau de Bure, the IF frequency $\nu_{IF}$ is 3 GHz, and a 1 % loss is obtained as soon as the delay tracking error would be 7.5 picoseconds, i.e. a geometrical shift of 2.2 mm only. Due to Earth rotation, the geometrical delay changes by such an amount in 0.1 s for a 300 m baseline. Hence, delay tracking would have to be done quite fast to avoid sensitivity losses. To avoid this problem, it is common to use sideband separation. The delay tracking error should then be kept small compared to the bandwidth of each spectral channel, $\tau_g \ll 1/\Delta\nu$, and the delay can then be adjusted much less frequently.

## 2.4   Fringe Stopping and Complex Correlator

With the Earth rotation, the cosine term of Eq.2.22 modulates the correlator output quasi-sinusoidaly with a *natural fringe rate* of

$$\nu_{LO}d\tau_g/dt \quad \simeq \quad \Omega_{earth}b\nu_{LO}/c \tag{2.27}$$

which is of order of 10 Hz for b= 300 m baselines and $\nu_{LO}$ = 100 GHz, or 2″ angular resolution (since the fringe rate only depends on the effective angular resolution).

The fringe rate is somewhat too high for simple digital sampling of the visibility. An exception is VLBI (because there is no other choice), although the resolutions are < 1 mas. The usual technique is to modulate the phase of the `local oscillator` $\Phi_{LO}$ such that $\Phi_{LO}(t) = 2\pi\nu_{LO}\tau_g(t)$ at any given time. Then

$$r_r = A_o|V|\cos(\pm 2\pi\nu_{IF}\Delta\tau - \Phi_V) \tag{2.28}$$

(with the $+$ sign for USB conversion, and the $-$ sign for LSB conversion), is a slowly varying output, which would be constant for a point source at the reference position (or delay tracking center). This process is called *Fringe Stopping*. After fringe stopping, we can no longer measure the amplitude $|V|$ and the phase $\Phi_V$ separately. A second correlator, with one signal phase shifted by $\pi/2$ becomes necessary. Its output is

$$r_i = A_o |V| \sin(\pm 2\pi \nu_{IF} \Delta\tau - \Phi_V) \tag{2.29}$$

With both correlators, we measure directly the real $r_r$ and imaginary $r_i$ parts of the complex visibility $r$. The device is thus called a **"complex" correlator**.

**Note:** A delay tracking error $\Delta\tau$ appears as a phase slope as a function of frequency, with

$$\Phi(\nu_{IF}) = \pm 2\pi \nu_{IF} \Delta\tau \tag{2.30}$$

## 2.5 Fourier Transform and Related Approximations

The *Complex Visibility* is

$$V = |V|e^{i\Phi_V} = \int_{Sky} A(\sigma)I(\sigma)e^{(-2i\pi\nu \mathbf{b}.\sigma/c)}\, d\Omega \tag{2.31}$$

Let $(u, v, w)$ be the coordinate of the baseline vector, in units of the observing wavelength $\nu$, in a frame of the phase tracking vector $\mathbf{s_0}$, with $w$ along $\mathbf{s_0}$. $(x, y, z)$ are the coordinates of the source vector $\mathbf{s}$ in this frame. Then

$$\begin{aligned}
\nu\mathbf{b}.\mathbf{s}/c &= ux + vy + wz \\
\nu\mathbf{b}.\mathbf{s_0}/c &= w \\
z &= \sqrt{1 - x^2 - y^2} \\
\text{and} \quad d\Omega &= \frac{dx\,dy}{z} = \frac{dx\,dy}{\sqrt{1 - x^2 - y^2}}
\end{aligned} \tag{2.32}$$

Thus,

$$V(u, v, w) = \int_{-\infty}^{+\infty} \int_{-\infty}^{+\infty} A(x, y)I(x, y)e^{-2i\pi\{ux+vy+w(\sqrt{1-x^2-y^2}-1)\}} \frac{dx\,dy}{\sqrt{1 - x^2 - y^2}} \tag{2.33}$$

with $I(x, y) = 0$ when $x^2 + y^2 \geq 1$.

If $(x, y)$ are sufficiently small, we can make the approximation

$$(\sqrt{1 - x^2 - y^2} - 1)w \simeq \frac{1}{2}(x^2 + y^2)w \simeq 0 \tag{2.34}$$

and Eq.2.33 becomes

$$\begin{aligned}
V(x, y) &= \iint A'(x, y)I(x, y)e^{-2i\pi(ux+vy)}\, dx\,dy \tag{2.35} \\
\text{with} \quad A'(x, y) &= \frac{A(x, y)}{\sqrt{1 - x^2 - y^2}} \tag{2.36}
\end{aligned}$$

i.e. basically a 2-D Fourier Transform of $AI$, but with a phase error term $\pi(x^2 + y^2)w$. Hence, on limited field of views, the relationship between the sky brightness (multiplied by the antenna power pattern) and the visibility reduces to a simple 2-D Fourier transform.

There are other approximations related to field of view limitations. Let us quantify these approximations.

- **2-D Fourier Transform**
  We can further neglect the phase error term in Eq.2.36, if the condition

  $$|\pi(x^2 + y^2)w| << 1 \tag{2.37}$$

  is fulfilled. Now, note that

  $$w < w_{max} \simeq \frac{b_{max}}{\lambda} \simeq \frac{1}{\theta_s} \tag{2.38}$$

  where $Beam_s$ is the synthesized beam width. Thus, if $\theta_t$ is the field of view to be synthesized, the maximum phase error is

  $$\Delta\phi = \frac{\pi\theta_t^2}{4\theta_s} \tag{2.39}$$

  Using $\Delta\phi < 0.1$ radian (6°) as an upper limit (note that this is the maximum phase error, i.e. the mean phase error is much smaller) result in the condition (with all angles in radian...):

  $$\theta_t < \frac{1}{3}\sqrt{\theta_s} \tag{2.40}$$

- **Bandwidth Smearing**
  Assume $u, v$ are computed for the center frequency $\nu_0$. At frequency $\nu_0$, we have

  $$V(u, v) \rightleftharpoons AI(x, y) \tag{2.41}$$

  The similarity theorem on Fourier pairs give

  $$V(\frac{\nu_0}{\nu}u, \frac{\nu_0}{\nu}v) = (\frac{\nu}{\nu_0})^2 I(\frac{\nu}{\nu_0}x, \frac{\nu}{\nu_0}y) \tag{2.42}$$

  Averaging over the bandwidth $\Delta\nu$, there is a *radial smearing* equal to

  $$\sim \frac{\Delta\nu}{\nu_0}\sqrt{x^2 + y^2} \tag{2.43}$$

  and hence the constraint

  $$\sqrt{x^2 + y^2} \le 0.1\frac{\theta_s\nu_0}{\Delta\nu} \tag{2.44}$$

  if we want that smearing to be less than 10% of the synthesized beam.

- **Time Averaging**
  Assume for simplicity that the interferometer observes the Celestial Pole. The baselines cover a sector of angular width $\Omega_e\Delta t$, where $\Omega_e$ is the Earth rotation speed, and $\Delta t$ the integration time. The smearing is *circumferential* and of magnitude $\Omega_e\Delta t\sqrt{x^2 + y^2}$, hence the constraint

  $$\sqrt{x^2 + y^2} \le 0.1\frac{\theta_s}{\Omega_e\Delta t} \tag{2.45}$$

  For other declinations, the smearing is no longer rotational, but of similar magnitude.

To better fix the importance of such approximations, the relevant values for the Plateau de Bure interferometer are given in Table 2.1. Note that these fields of view correspond to a maximum phase error of 6° only, or to a (one dimensional) distortion of a tenth of the synthesized beam, and thus are not strict limits. In particular, atmospheric errors often results in larger errors (which are independent of the field of view, however).

## 2.6   Array Geometry & Baseline Measurements

| Config. | Resolution | Frequency (GHz) | 2-D Field | 0.5 GHz Bandwidth | 1 Min Time Averaging | Primary Beam |
|---------|-----------|-----------------|-----------|-------------------|----------------------|--------------|
| Compact | 5″ | 80 GHz | 5′ | 80″ | 2′ | 60″ |
| Standard | 2″ | 80 GHz | 3.5′ | 30″ | 45″ | 60″ |
| Standard | 2″ | 220 GHz | 3.5′ | 1.5′ | 45″ | 24″ |
| High | 0.5″ | 230 GHz | 1.7′ | 22″ | 12″ | 24″ |

Table 2.1: Field of view limitations as function of angular resolution and observing frequency for the Plateau de Bure interferometer.

$uv$ **coverage**   Using a Cartesian coordinate system $(X, Y, Z)$ with $Z$ towards the pole, $X$ towards the meridian, and $Y$ towards East, the conversion matrix to $u, v, w$ is

$$\begin{pmatrix} u \\ v \\ w \end{pmatrix} = \frac{1}{\lambda} \begin{pmatrix} \sin(h) & \cos(h) & 0 \\ -\sin(\delta)\cos(h) & \sin(\delta)\cos(h) & \cos(\delta) \\ \cos(\delta)\cos(h) & -\cos(\delta)\sin(h) & \sin(\delta) \end{pmatrix} \begin{pmatrix} X \\ Y \\ Z \end{pmatrix} \tag{2.46}$$

where $h, \delta$ are the hour angle and declination of the phase tracking center.
Eliminating $h$ from Eq.2.46 gives the equation of an ellipse:

$$u^2 + \left( \frac{v - (Z/\lambda)\cos(\delta)}{\sin(\delta)} \right)^2 = \frac{X^2 + Y^2}{\lambda^2} \tag{2.47}$$

The $uv$ coverage is an ensemble of such ellipses. The choice of antenna configurations is made to cover the $uv$ plane as much as possible.

**Baseline measurement**   Assume there is a small baseline error, $(\Delta X, \Delta Y, \Delta Z)$. The phase error is

$$\Delta\phi \quad = \quad \frac{2\pi}{\lambda} \Delta \mathbf{b}.\mathbf{s}_0 \tag{2.48}$$

$$= \quad \cos(\delta)\cos(h)\Delta X - \cos(\delta)\sin(h)\Delta Y + \sin(\delta)\Delta Z \tag{2.49}$$

Hence, if we observe $N$ sources, we have for each source

$$\phi_k = \phi_0 + \cos(\delta_k)\cos(h_k)\Delta X - \cos(\delta_k)\sin(h_k)\Delta Y + \sin(\delta_k)\Delta Z \tag{2.50}$$

i.e. a linear system in $(\Delta X, \Delta Y, \Delta Z)$, with $N$ equations and 4 unknown (including the arbitrary phase $\phi_0$). This can be used to determine the baselines from phases measured on a set of sources with known positions $h_k, \delta_k$.

From the shape of Eq.2.49, one can see that the determination of $\Delta X, \Delta Y$ requires large variations in $h$, preferably at declination $\delta \sim 0$, while that of $\Delta Z$ requires large variations in $\delta$. However, $\phi_k$ in Eq.2.50 is multi-valued (the $2\pi$ ambiguity...). Hence, the system to solve is in fact

$$mod(\phi_0 + \cos(\delta_k)\cos(h_k)\Delta X - \cos(\delta_k)\sin(h_k)\Delta Y + \sin(\delta_k)\Delta Z - \phi_k, 2\pi) = 0 \tag{2.51}$$

which is a linear system of equations only if $\Delta X, \Delta Y, \Delta Z$ are small enough so that the modulo function is the identity. Baseline determination usually proceeds through a "brute force" technique, by making a grid search around the most likely values for $X, Y, Z$.